SAND-96--0076C
SAND96-0781C
CONF-960502--2

DRY ETCH DEVELOPMENT OF W/WSi SHORT GATE MESFETs

R. J. Shul, M. E. Sherwin, A. G. Baca, J. C. Zolper, D. J. Rieger, and R. D. Briggs
Sandia National Laboratories, Albuquerque, New Mexico 87185-0603

Refractory metal thin films are often used in the fabrication of high-speed GaAs field effect transistors (FETs) as Schottky contacts. Tungsten (W) and tungsten silicide (WSi_x) can be utilized in a self-aligned gate process as an ion implantation mask during the formation of source and drain regions for metal-semiconductor FETs (MESFETs). The gate etch must be highly anisotropic to accurately define the implant region. In this paper we report the fabrication of sub-0.5 μm W/WSi_x bilayer gates using electron beam lithography and dry etch techniques. Reactive ion etching (RIE) and high-density electron cyclotron resonance (ECR) etch processes are compared for W and WSi_x etch rates and etch profiles.

INTRODUCTION

The use of refractory metal thin films in the fabrication of high-speed, high-density GaAs field effect transistors (FETs) are prominent with applications as interconnects, via plugs, and ohmic and Schottky contacts. The fabrication of metal-semiconductor FETs (MESFETs) often incorporates W and/or WSi_x gate features as a self-aligned ion implantation mask to form source and drain regions. The gate etch profile must be highly anisotropic to accurately define the implant region. As device design rules shrink to sub-0.5 μm gate lengths, the etch requirements and patterning techniques become even more critical.

Tungsten and tungsten silicide thin films have been etched in reactive ion etch (RIE) systems using fluorine-containing plasmas [1-6] including; SF_6, CF_4, CHF_3, and NF_3. Both NF_3- and SF_6-based plasmas show enhanced etch rates due to less polymer formation than plasma chemistries containing carbon. Etch rates and the fluorine atom concentrations increase with the addition of N_2 [7] or O_2 [8]. Due to the substantial chemical etch of W or WSi_x in fluorinated plasmas, lateral etching of the exposed sidewalls often results in concave etch profiles. The undercut can be so severe that critical dimensions are not maintained and gate profiles do not properly align to the ion implant region producing poor device characteristics. Additionally, concave sidewalls can prevent good step coverage with passivating dielectric films deposited over the gates; thus reducing long term reliability of the device.

Anisotropic etching with straight wall profiles is often obtained when an involatile film is deposited on the sidewall of the etched feature. The use of fluorocarbon plasma discharges (CF_4, CHF_3, etc.) often results in the formation of sidewall polymers which impede the lateral etching of the W or WSi_x feature [4]. Vertical etching has also been reported at low-temperatures [6, 9] due to reduced reactivity of the W and WSi_x with F. Fullowan et *al.* have reported highly anisotropic etching of W in SF_6- and CF_4-based plasmas with the use of a Ti mask [5]. They have proposed the formation of an involatile

TiF_3 film which forms on the sidewall and minimizes lateral etching. Anisotropy may also be increased by increasing the acceleration of energetic ions from the plasma to the surface. However, this energetic ion bombardment of the surface can damage the sample and degrade electrical device performance. Attempts to minimize such damage by reducing the ion energy or increasing the chemical activity in the plasma often results in a loss of etch rate or anisotropy which significantly limits critical dimensions and reduces the utility of the process for vertical etch profiles. It is therefore necessary to develop plasma etch processes for W and WSi_x which couple anisotropy for critical dimension and sidewall profile control and high etch rates with low-damage for optimum device performance.

A great deal of interest has been generated in low-damage etch processes based on high-density-plasmas, such as electron cyclotron resonance (ECR) plasmas and inductively coupled plasmas (ICP). Due to the magnetic confinement of electrons in the microwave ECR source, high density plasmas are formed at low pressures with low plasma potentials and ion energies. Therefore, less damage than that produced by RIE plasmas has been observed during ECR etching of III-V materials [12-17]. Ion densities in excess of 5×10^{11} cm^{-3} are achieved thereby increasing the potential etch rate due to higher ion flux. Highly anisotropic etching can be achieved in the ECR by superimposing an rf-bias (13.56 MHz) on the sample and employing low pressure conditions to minimize ion scattering which contributes to lateral etching. With rf-biasing, energetic ions are accelerated from the plasma to the sample with potential for kinetic damage to the surface; however, sidewall damage may be low due to the directional nature of the beam, the chemical component of the etch, and the low process pressure

The refractory gate materials used in a self-aligned process are typically W, WSi_x, or a W/WSi_x bilayer structure. In the composition range of $x = 0.4$ to 0.5, WSi_x remains amorphous up to 875°C and is a better diffusion barrier and Schottky contact than W [18]. The use of a W/WSi_x bilayer gate improves gate resistance while maintaining a good Schottky contact to GaAs [19]. Furthermore, conductivity is improved by using W as the top layer, which at 20 μΩ-cm is a factor of 10 more conductive than WSi_x. The underlying WSi_x is used as the Schottky contact to GaAs. Use of a bilayer gate structure complicates the etch since WSi_x tends to etch faster than W and undercuts more due to the high lateral etch rate. This may not effect device performance if the upper layer W etch feature is anisotropic and accurately defines the ion implant area.

We have investigated the etch rates and profiles for W, WSi_x, and W/WSi_x bilayer films as a function ECR and RIE etch conditions. Plasma chemistry, pressure, rf power, and microwave power were studied. Etch conditions were optimized and applied to W/WSi_x bilayer MESFET structures.

EXPERIMENTAL

Tungsten, WSi_x, and W/WSi_x bilayer films were deposited using a DC magnetron sputtering system at 10 mT with an Ar flow rate of 30 sccm and a power of 1005 W. The W films were 3000 Å thick with a resistivity of 20 μΩ-cm, the WSi_x films were 4000 Å thick with a resistivity of 180 to 200 μΩ-cm, and the bilayer gate consisted of 2000 Å of W deposited over 2000 Å of WSi_x with a combined resistivity of ~38 μΩ-cm. Gate features were patterned using a JEOL JBX5-FE electron-beam lithography system with a beam current of 285 pA and a spot size of 20 nm. Gates with lengths from 2.0 μm to 0.3 μm

were patterned in 5500Å of SAL-603 negative resist. Exposure doses were varied from a minimum of 12 $\mu C/cm^2$ for the 2.0 μm devices to a maximum of 28 $\mu C/cm^2$ for the 0.3 μm devices. Samples were baked at 105°C for 60 seconds immediately after exposure and then developed in MIF-312 CD-27 for 2 minutes.

RIE plasmas were generated in a 13.56 MHz rf-powered parallel plate Plasma-Therm Batchtop RIE system. Gases were distributed through a showerhead arrangement located in the upper electrode. The lower electrode was 17.8 cm in diameter with an interelectrode spacing of approximately 10 cm and was completely covered with a 3.2 mm thick quartz plate. Samples were attached to the quartz plate with a low-vapor-pressure thermal paste to ensure good thermal conduction. All RIE etches were done at 50°C.

The ECR plasma reactor used in this study was a load-locked Plasma-Therm SLR 770 etch system with an ECR source operating at 2.45 GHz. Ion energies were provided by superimposing an rf-bias (13.56 MHz) on the sample. Samples were mounted on an anodized Al carrier that was clamped to the cathode and cooled with He gas. Gases were introduced through an annular ring into the chamber just below the quartz window. To minimize field divergence and optimize plasma uniformity and ion density across the chamber, an external secondary collimating magnet was located on the same plane as the sample and a series of external permanent rare-earth magnets were located between the microwave cavity and the sample. All ECR etches were done at 10°C.

Etch rates for samples exposed to the RIE plasma were calculated from optical endpoint using laser reflectometry. Error bars for RIE etch rates were estimated at ± 10%. Etch rates from samples etched in the ECR were calculated from the depth of etched features measured with a Dektak stylus profilometer following photoresist removal with acetone. Depth measurements were taken at a minimum of three positions. Error bars for the ECR etch rates represent the standard deviation of the etch depth across the sample. Several plasma conditions were repeated with better than ±10% sample-to-sample variation. Surface morphology, anisotropy, and sidewall undercutting were evaluated with a scanning electron microscope (SEM).

RESULTS AND DISCUSSION

RIE etch rates for W, WSi_x, and W/WSi_x are shown in Figure 1 as a function of pressure. In general, the etch rates increased as the pressure was increased implying a reactant limited regime at low pressure. The W etch rate decreased at 25 mTorr possibly due to increased deposition on the etch surface. In Figure 2, ECR etch rates for W and WSi_x are shown as a function of pressure. During these runs the rf-power was held constant at 50 W which resulted in an increase in dc-bias as the pressure was increased. Higher dc-biases are attributed to increased collisional recombination which decreases the plasma density at higher pressures. The W etch rates increased as the pressure was increased from 1 to 5 mTorr suggesting a reactant limited regime at low pressure. As the pressure was increased above 5 mTorr, the etch rates remained relatively constant due either to lower ion densities or to increased deposition at higher pressures. The WSi_x etch rates showed a similar trend however a significant decrease was observed at 3 mTorr.

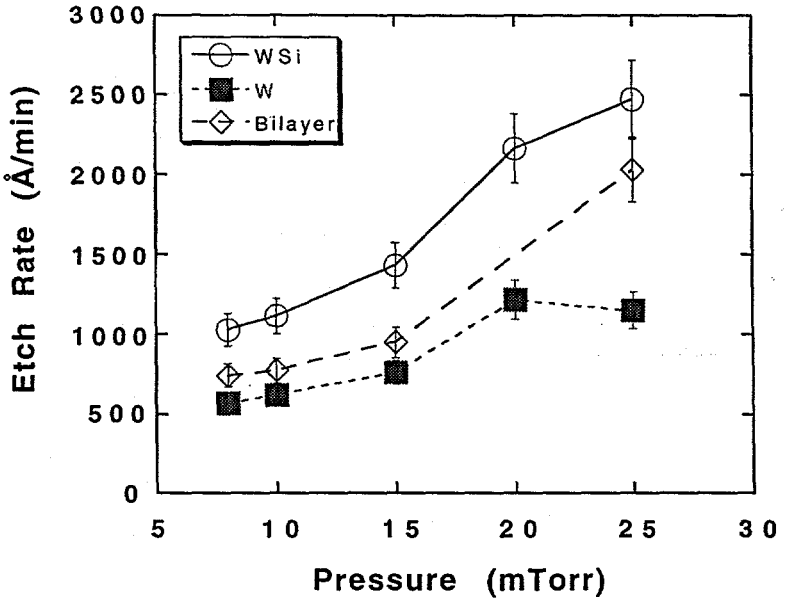

Figure 1. Etch rates for W, WSi_x, and W/WSi_x as a function of pressure for an RIE generated SF_6/Ar plasma (2.5 sccm/10 sccm) at 50 W rf power.

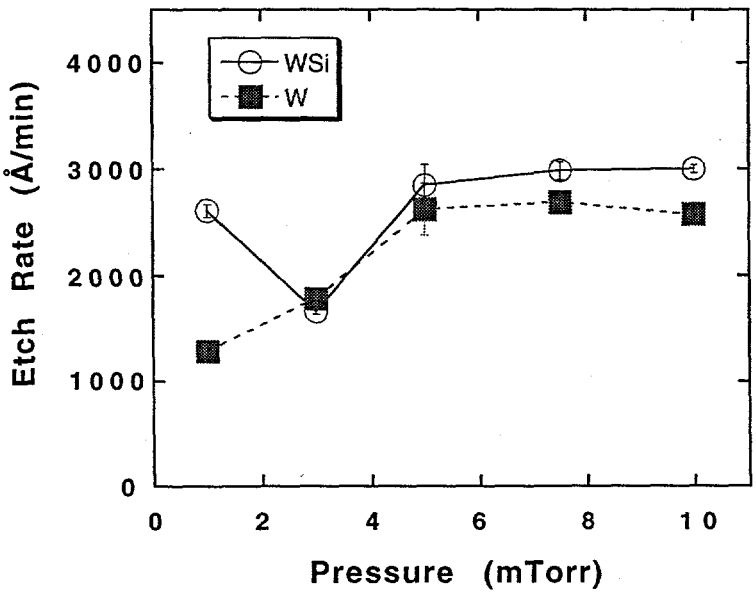

Figure 2. Etch rates for W and WSi_x as a function of pressure for an ECR generated SF_6/Ar plasma (5 sccm/20 sccm) at 500 W microwave power and 50 W rf power.

In Figure 3, W, WSi_x and W/WSi_x etch rates in the RIE are shown as a function of rf power. The etch rates increased as the rf power increased due to higher ion-bombardment energies. ECR etch rates for W and WSi_x (Figure 4) increased as the rf power was increased from 1 to 150 W and then decreased slightly at 300 W. The decrease at 300 W may be attributed to sputter desorption of active species before they have time to react at the semiconductor surface. In Figure 5, W and WSi_x etch rates are shown as a function of ECR microwave power. The etch rates increased dramatically with the application of microwave power due to the increase in ion density and reactive F. Etching was less than 175 Å/min for both W and WSi_x in the RIE-mode (without applied microwave power) during the 1 minute exposure time. The etch rates tend to remain relatively constant as the microwave power was increased above 500 W possibly due to saturation of reactive F in the plasma.

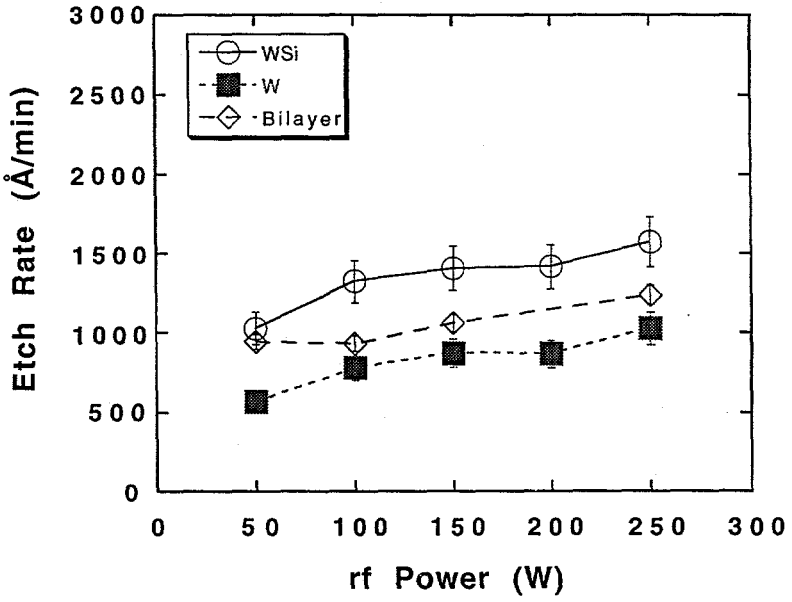

Figure 3. Etch rates for W, WSi_x, and W/WSi_x as a function of rf power for an RIE generated SF_6/Ar plasma (2.5 sccm/10 sccm) at 8 mTorr pressure.

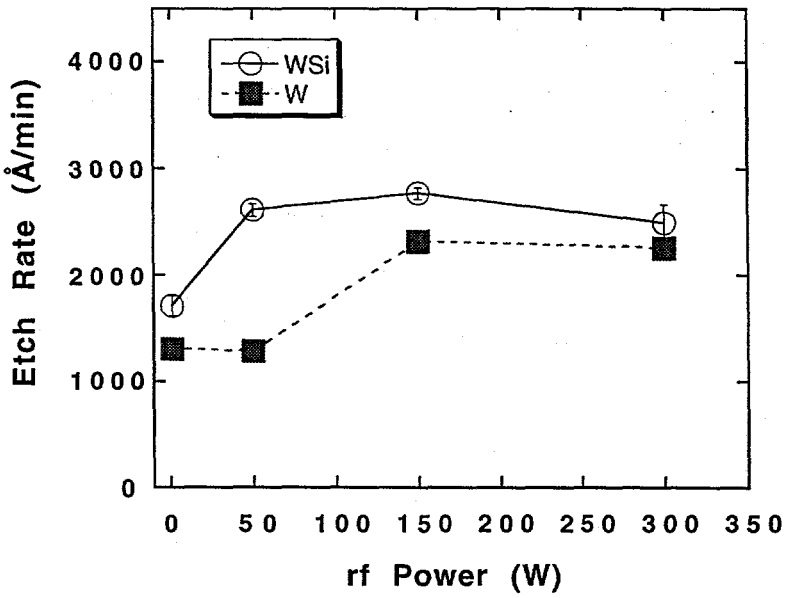

Figure 4. Etch rates for W and WSi_x as a function of rf power for an ECR generated SF_6/Ar plasma (5 sccm/20 sccm) at 500 W microwave power and 1 mTorr pressure.

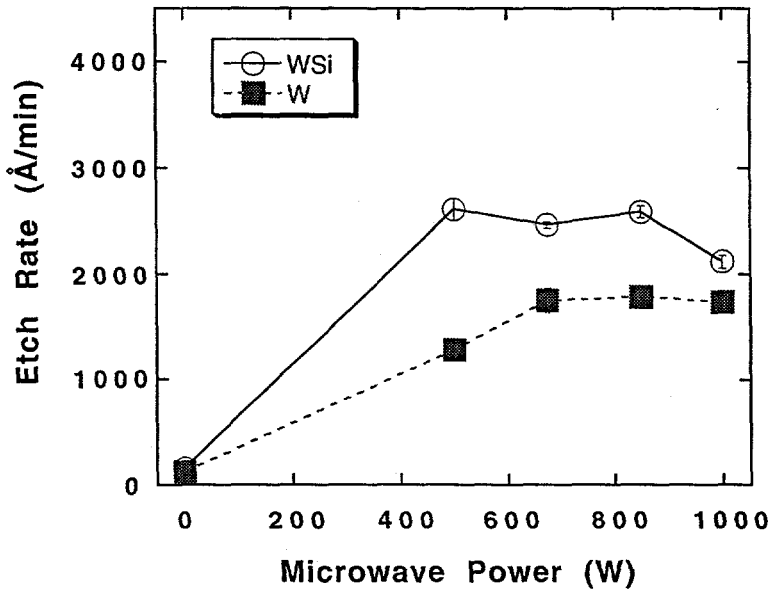

Figure 5. Etch rates for W and WSi_x as a function of microwave power for an ECR generated SF_6/Ar plasma (5 sccm/20 sccm) at 1 mTorr pressure and 50 W rf power.

The W and WSi etches are very chemical in nature and show a very strong dependence on plasma chemistry as seen in Figures 6 to 8. In Figure 6, W, WSi_x and W/WSi_x etch rates are shown as a function of SF_6 flow in a RIE-generated SF_6/Ar plasma. The etch rates increased as the SF_6 concentration increased due to higher concentrations of reactive F. Similarly, the W and WSi_x etch rates increased as the SF_6 flow was increased in the ECR-generated SF_6/Ar plasma (Figure 7). Etch rates in the ECR were a factor of 2 to 4 greater than those etched in the RIE due to the higher ion densities and reactive F concentrations generated in the ECR. In Figure 8, etch rates are shown as a function of CHF_3 flow in a RIE SF_6/Ar plasma. CHF_3 was not included in the study of the ECR plasma due to the possibility of C deposition on the chamber walls. As the CHF_3 concentration was increased above approximately 8% the etch rates decreased possibly due to increased polymer deposition on the surface which minimized chemical etching.

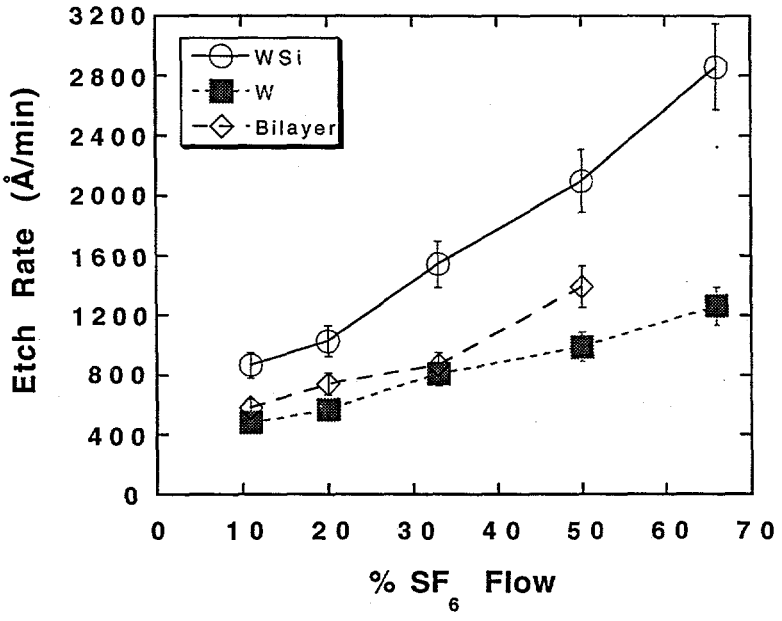

Figure 6. Etch rates for W, WSi_x, and W/WSi_x as a function of $\%SF_6$ flow for an RIE generated SF_6/Ar plasma (10 sccm Ar) at 8 mTorr pressure and 50 W rf power.

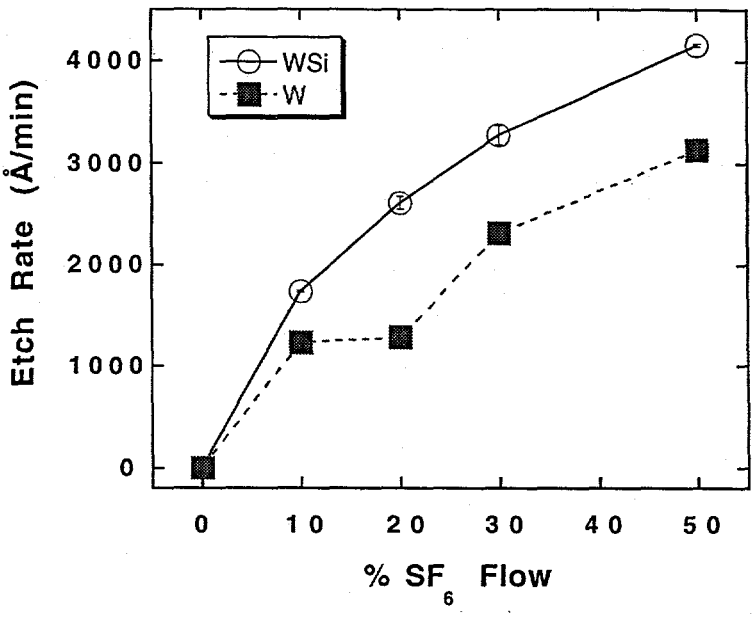

Figure 7. Etch rates for W and WSi_x as a function of $\%SF_6$ flow for an ECR generated SF_6/Ar plasma (20 sccm Ar) at 1 mTorr pressure, 50 W rf power and 500 W microwave power.

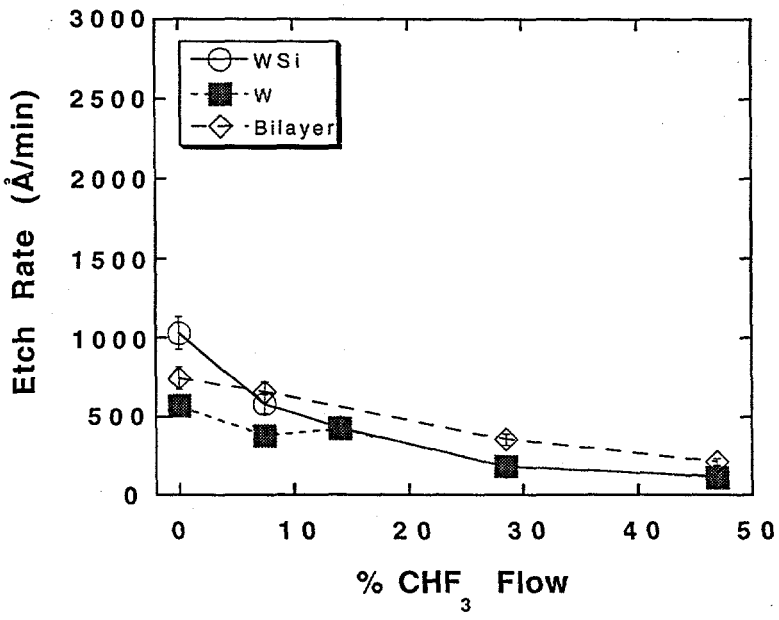

Figure 8. Etch rates for W, WSi_x, and W/WSi_x as a function of $\%CHF_3$ flow for a RIE generated CHF_3/SF_6/Ar plasma (2.5 sccm SF_6 and 10 sccm Ar) at 8 mTorr pressure and 50 W rf power.

In this study, WSi_x typically etched faster than W. We have also observed significant undercut of both W and WSi_x in the RIE and ECR plasmas as the pressure or SF_6 concentration was increased. The etch profiles were more isotropic under these conditions due to increased lateral etching of the refractory metal at higher F concentrations. This is consistent with the strong chemical component of the etch mechanism. The WSi_x undercut was more substantial due to the higher etch rates. Etch rates were consistently higher in the ECR under comparable conditions for W and WSi_x due to higher ion densities and concentrations of reactive F generated in the ECR. However, we did not observe any significant advantages in the etch profile or surface morphology using the ECR. The RIE system was used to etch W/WSi_x MESFET gates under moderate dc-bias conditions, low pressure, and low SF_6 flows.

BILAYER SHORT GATE DEVICES

In Figure 9a, a 0.4 μm W/WSi_x gate is shown as etched in a RIE-generated SF_6/Ar plasma. The plasma conditions were; 2.5 sccm SF_6, 10 sccm Ar, 50 W rf power, and 8 mTorr pressure. The etch rate of the combined W/WSi_x film was 840 ± 50 Å/min. A 10%

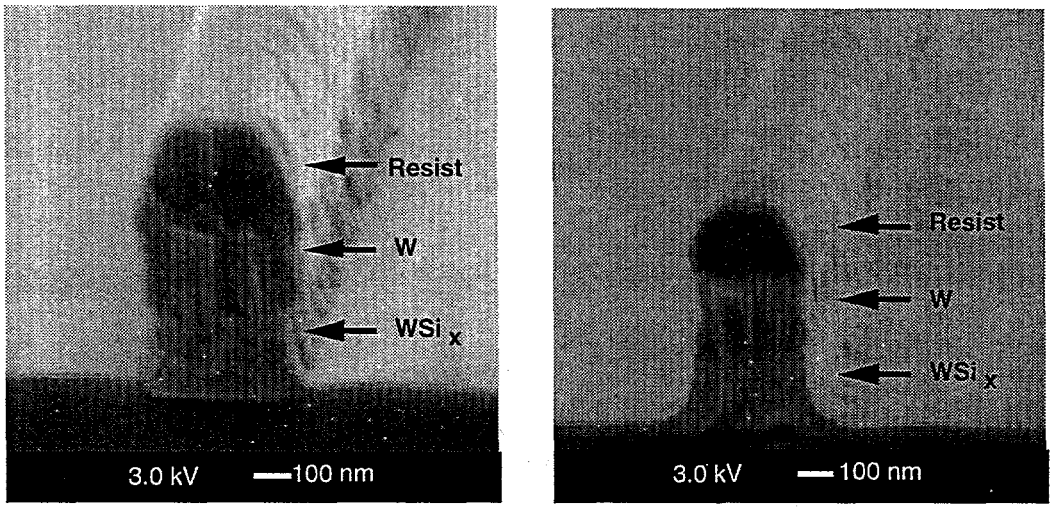

(a) (b)

Figure 9. SEM micrograph of 0.4 μm W/WSi gates etched in (a) SF_6/Ar and (b) $SF_6/CHF_3/Ar$ RIE discharge at 50 W rf-power and 8 mTorr pressure.

overetch was used to assure complete removal of the W/WSi_x across the sample. During the overetch the GaAs was exposed to the plasma and sputtered at rates in excess of 50 Å/min. Therefore, it was critical that the ion energy was set to minimize the GaAs sputter rate, but also promote anisotropic etching. The pressure and SF_6 flow rate were low to minimize lateral etching without excessively reducing the etch rate. The gate profile showed some undercutting of the WSi_x film, however the W profile was quite anisotropic. The GaAs field was smooth while some vertical striations from the mask were observed in the W/WSi_x sidewall. In Figure 9b, a 0.4 μm W/WSi_x gate was etched under identical conditions with the addition of 5 sccm CHF_3. The etch was more anisotropic for the WSi_x

profiles and reduce damage to the etched surface. Process pressure and SF_6 flows were minimized to enhance the anisotropic profile of the gate and maintain reasonable etch rates. CHF_3 promoted etch anisotropy at the cost of reproducibility and lower etch rates and was eliminated from the etch chemistry

ACKNOWLEDGMENTS

The authors would like to thank A. T. Ongstad, P. L. Glarborg, and D. Tibetts-Russell for their technical support. This work was performed at Sandia National Laboratories supported by the U.S. Department of Energy under contract #DE-AC04-94AL85000.

REFERENCES

[1] T. D. Bestwick and G. S. Oehrlein, J. Appl. Phys., **66**, 5034 (1989).

[2] W. S. Pan and A. J. Steckl, J. Vac. Sci. Technol. **B6**, 1073 (1988).

[3] C.C. Tang and D. W. Hess, J. Electrochem. Soc., **131**, 115 (1984).

[4] M. L. Schattenburg, L. Plotnik, and H. I. Smith, J. Vac. Sci. Technol. **B6**, 1073 (1988).

[5] T. R. Fullowan, S. J. Pearton, F. Ren, G. E. Mahoney, and R. L. Kostelak, Semicond. Sci. Technol., **7**, 1489 (1992).

[6] C. W. Jurgensen, R. R. Kola, A. E. Novembre, W. W. Tai, J. Frackoviak, L. E. Trimbel, and G. K. Cellar, J. Vac. Sci. Technol., **B9**, 3280 (1991).

[7] N. Mutsukura and G. Turban, J. Electrochem. Soc. **137**, 225 (1990).

[8] J.N. Randall and J. C. Wolfe,. Appl. Phys. Lett., **39**, 742 (1981).

[9] S. Tachi, K. Tsujimoto, S. Arai, and T. Kure, J. Vac. Sci. Technol., **A9**, 796 (1991).

[10] R. J. Shul, D. J. Rieger, A. G. Baca, C. Constantine, and C. Barratt, Electron. Lett., **30**, 84 (1994).

[11] R. J. Shul, A. G. Baca, D. J. Rieger, and A. J. Howard, Electron. Lett., **31**, 317 (1995).

[12] C. Constantine, D. Johnson, S. J. Pearton, U. K. Chakrabarti, A. B. Emerson, W. S. Hobson, and A. P. Kinsella, J. Vac. Sci. Technol. **B 8**, 596 (1990).

[13] S. J. Pearton, U. K. Chakrabarti, A. P. Kinsella, D. Johnson, and C. Constantine, Appl. Phys. Lett. **56**, 1424 (1990).

[14] A. J. Murrell, R. C. Grimwood, P. O'Sullivan, M. Gilbert, K. Vanner, F. Ruddell, I. Davies, K. Hilton, S. Bland, and D. Spear, Technical Digest, Proc. 1992 GaAs IC Symposium, 173.

[15] R. Cheung, Y. H. Lee, K. Y. Lee, T. P. Smith, III, D. P. Kern, S. P. Beaumont, and C. D. W. Wilkinson, J. Vac. Sci. Technol. **B 7**, 1462 (1989).

[16] K. K. Ko and S. W. Pang, J. Electrochem. Soc. **141**, 250 (1994).

[17] R. J. Shul, M. L. Lovejoy, A. G. Baca, J. C. Zolper, D. J. Rieger, M. J. Hafich, R. F. Corless, and C. B. Vartuli, J. Vac. Sci. Technol., **A13**, 912 (1995).

[18] A. G. Lahav, C. S. Wu, and F. A. Biaocchi, , J. Vac. Sci. Technol., **B6**, 1785 (1988).

[19] M. Kanamori, K. Nagai, and T. Nozaki, , J. Vac. Sci. Technol., **B5**, 1317 (1987).

[20] C. Constantine, private communication.

[19] M. Kanamori, K. Nagai, and T. Nozaki, , J. Vac. Sci. Technol., **B5**, 1317 (1987).

[20] C. Constantine, private communication.

KEYWORDS

1. Refractory metal gates, page 1, 2,
2. ECR etching, page 1, 2, 3, 4, 5, 6, 7, 8, 11
3. RIE etching, page 1, 2, 3, 4, 5, 6, 7, 8, 11
4. MESFETs, page 1
5. Self-aligned gate technology, page 1, 2
6. Etch profile, page 9, 11
7. Cutoff frequency, page 10

DISCLAIMER